Journal of Non-Oxide Glasses Vol. 6, No 3, 2014, p. 53 - 60

SYNTHESIS AND TRIBOLOGICAL PROPERTIES OF FLOWER-LIKE MoS_2 NANOSTRUCTURES

J. XU[a,b], H. TANG[a,b], K. ZHANG[b], H. ZHANG[b], C. LI[a,b*]

[a]*School of Materials Science and Engineering, Jiangsu University, Zhenjiang,212013, Jiangsu Province, China*

[b]*Key Laboratory of Tribology of Jiangsu Province, Zhenjiang 212013, Jiangsu Province, China*

Spherical molybdenum disulfide (MoS2) aggregates composed of ultrathin nanoplates with size of 10 nm were successfully synthesized via a facile solid-sate reaction. The structure and morphology of the as-prepared products were characterized by X-ray powder diffraction, energy dispersive spectroscopy, scanning electron microscopy and transmission electron microscopy. In addition, the tribological properties of the as-prepared MoS2 powders as additives in the HVI500 base oil were investigated on an UMT-2 multi-specimen tribo-tester. The topography of worn scars was obtained using a common SEM. It was found that the addition of MoS2 nanospheres could improve the tribological properties of the base oil.

(Received May 8, 2014; Accepted July 25, 2014)

Keywords: MoS2, Solid-sate reaction, Tribological properties

1. Introduction

In recent years, interest in the synthesis and application of transition metal dichalcogenides MS2 (M: Mo, W) nanomaterial has steadily grown because of their unique structure and superior properties [1]. As we know, transition metal dichalcogenides have a sandwich interlayer structure formed by the stacking of the S–M–S layers, which are loosely bound to each other only by van der Waals forces and are easily cleaved [2]. Moreover, MS2 exhibits unique physical, optical and electrical properties correlated with their layer structure. In addition, their electronic structure is such that band-edge excitation corresponds largely to a metal centred d–d transition. Owing to these features, laminar MS2 materials have numerous applications such as solid lubricants, catalysis, lectrocatalysis, high-density batteries and efficient solar energy cells [3–6].

Molybdenum disulfide (MoS2) is one of the transitionmetal dichalcogenide layered compounds, has been used for decades in specialised applications as a solid lubricant or an additive for lubricating oils and greases. As a lubricant, MoS2 nanomaterials exhibit low friction coefficients and have a long lifetime in dry air, inert or vacuum environments [7]. To date, MoS2 nanomaterials have attracted considerable attention and have been synthesised by a great diversity of methods, for instance, gas-phase reactions, laser ablation, sonochemical process, hydrothermal synthesis and thermal decomposition [8–11].Therefore, much effort has been devoted to the synthesis of various nanoscale MoS2 with specific morphologies and unique properties. A large number of MoS2 nanoparticles with different morphologies such as nanowires [12], nanotubes [13-16], nanosheets [17,18], nanorods [19], and nanoflowers [15,20,21] have been prepared. Previous studies have shown that nanosized MoS2 such as nanorods and nanosheets usually have

*Corresponding author: lichangshengujs@yahoo.com

better tribological properties, either in friction reduction or wear resistance than bulk MoS2 [22].

In our previous research [23], MoS2 and MoS2 nanoflowers exhibited excellent tribological behaviour as a lubricant additive. However, MoS2 spherical-like self-assembled nanostructures and their application in the tribiological field have rarely been reported and not to mention its application in the tribological field. Herein, we report on the shape-selective synthesis of 3D MoS2 nanosphere by a facile solid-state reaction. The products were characterised by an X-ray diffractometer (XRD), an energy-dispersive X-ray spectrometer (EDS), scanning electron microscopy (SEM) and transmission electron microscopy (TEM). Moreover, the tribological properties of MoS2 nanosphere as additives in the HVI500 base oil were also investigated.

2. Experimental

All chemical reagents (analytical purity) were purchased from SCRC Chemical Co. and used directly without further purification. The experiment was designed by three different preparation samples of MoS2 in the following table 1:

Table1 Three different preparation samples of MoS_2: A,B,C

Sample A: 1g of MoO3	+	4.44g of sulfur powder
Sample B: 1 g of MoO3	+	10.55g of thiocarbamide
Sample C 1g of molybdenum powder	+	6.67g of sulfur powder

The three groups of mixture powders were energetically ball-milled at 400 rpm (rotation per minute) in the presence of ethanol for 12 h in a planetary ball mill respectively. Then the ball-milled mixture was introduced into 10-ml stainless steel reactor in a nitrogen-filled glove box. The filled reactor was tightly closed with the threaded plug and pushed into the tube furnace. The temperature of the tube furnace was raised to 820°C at a rate of 10°C /min and the heat was maintained at 820°C for 2h. Subsequently the reactor gradually cooled to room temperature, opened, and the black powders were obtained. The product was directly characterized without further processing by various analytic techniques.

The as-prepared MoS2 samples, were dispersed in paraffin base oil via 2 h ultrasonication without any active reagent, and then a series of suspended oil samples were obtained. The tribological properties of the base oil containing MoS2 samples were evaluated on a UMT-2 ball-on-plate friction. The testing of friction reduction and wear resistance was conducted at rotating speed of 300 rpm and load of 5-50 N for 30 min. The material of upper sample is 440C stainless steel ball with a diameter of 10 mm, hardness of 62 HRC, and the counterpart is 45 steel disc of Φ40 mm×3 mm in size. The friction coefficient was automatically recorded during the contact friction.

The X-ray diffraction (XRD) patterns were recorded using a D8 advance (Bruker-AXS) diffractometer with Cu *Ka* radiation (λ = 0.1546 nm). The 2θ range used in the measurement was from 10 to 80° with a velocity of 5°/min. The morphologies and structures of the samples were characterized by scanning electron microscopy (SEM, JEOL JXA-840A) and transmission electron microscopy (TEM) with a Japan JEM-100CX II transmission electron microscope.

3. Results and discussion

3.1 Structure and morphology characterization

The crystalline structure and phase purity of MoS_2 nanostructures (sample A) were confirmed by XRD. As shown in Fig. 1a , All labelled diffraction peaks can be indexed to those of the pure hexagonal phase of MoS_2 with lattice constants a = 3.161, c = 12.84 Å, which are in good agreement with the values of standard card (JCPDS No. 37-1492). No characteristic peaks were detected from other impurities, indicating that the sample was of high purity. Moreover, the XRD patterns reveal wide and weak diffraction peaks, which is evidence of the formation of nanoparticles. The EDS result (Fig. 1b) demonstrates that the MoS_2 nanoflowers consist of only elements Mo and S, and no other elements was observed. Furthermore, the quantification of the peaks shows that the atom ratio of Mo:S is about 1:1.98, which is close to 1:2 by the atomic ratio of MoS_2; hence the as-prepared product is a hexagonal MoS_2.

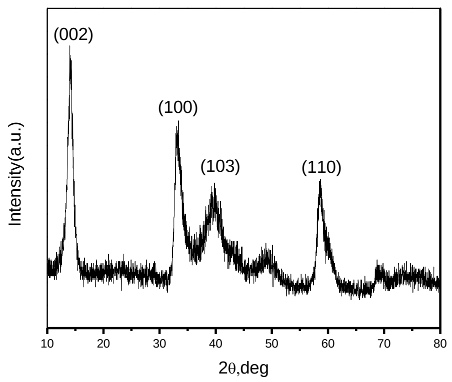

a

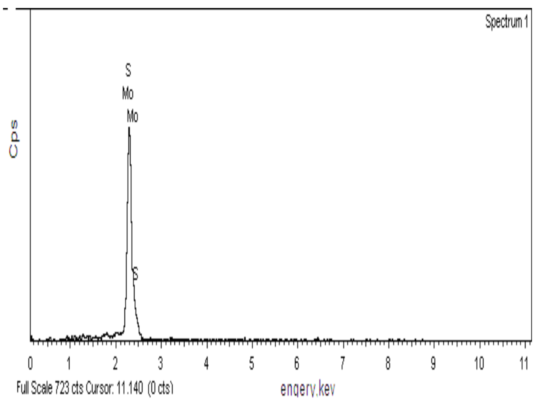

b

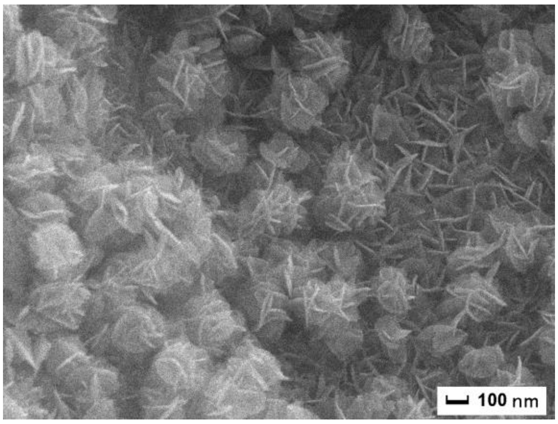

c

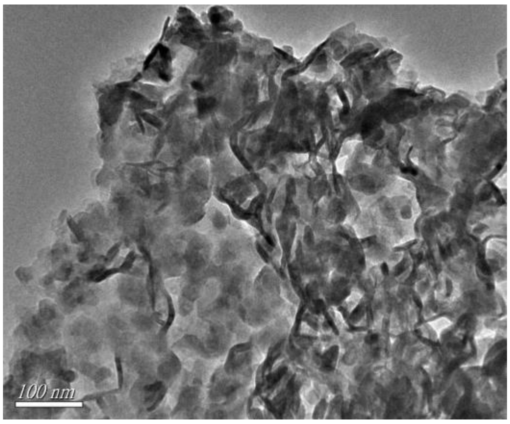

d

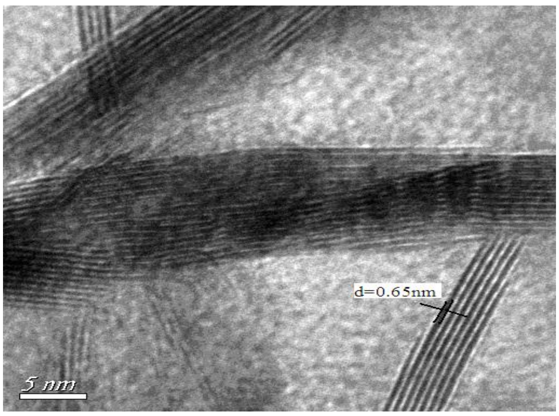

e

Fig. 1 XRD, SEM ,TEM and HRTEM images of the as-prepared MoS2 nanospheres(sample A)

a : XRD, b:EDS ,c:SEM ,d: TEM e: HRTEM

The size and morphologies of the spherical MoS_2 were primarily investigated by SEM measurement. Fig.1c indicates that the nanospheres are composed of MoS_2 nanosheets and shows that the size of the nanosphere is about 50–100 nm in size. Further, the highly wrinkled surface and extruded lamella-like structure of the spherical aggregates could be obviously observed. The morphology and structure of the as-synthesised MoS_2 products were further characterized using TEM. Fig.1d shows a typical TEM image of flower-like MoS_2 nanospheres, which further confirms the as-prepared MoS_2 nanospheres consist of many MoS_2 nanosheets. More details for MoS_2 structure are illustrated by HRTEM images in Fig.1e, which indicates that the nanosheets consist of about 6-layers structures. As a mean value, the distance between the lattice fringes is 0.65 nm, which is coincidental with the theoretical spacing for (002) planes of the hexagonal MoS_2 structure.

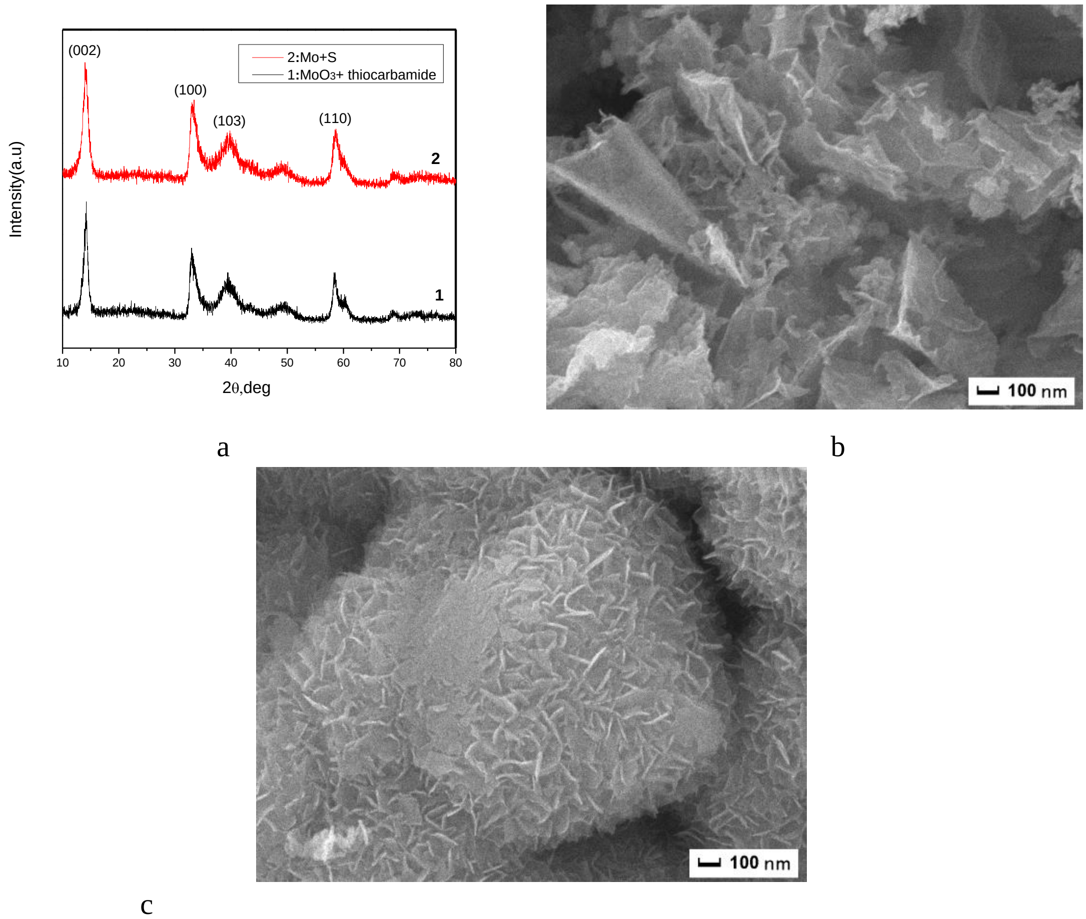

Fig. 2 XRD and SEM images of the as-prepared $_{MoS2}$ by preparation sample of B and C

a:XRD b nanosheets and c microspheres:SEM

In addition, precursors on the morphologies of the as-prepared MoS_2 product play an important role. The XRD patterns of sample B and sample C exhibit wide and weak diffraction peaks (Fig. 2a), indicating the formation of small MoS_2 nanoparticles. When MoO3 and thiocarbamide were used as reaction precursors, the obtained products were irregular plate-like structures (Fig. 2b). When Mo and S were adapted as precursors, uniform MoS_2 microspheres composed of nanosheets with an average diameter of about 500-800nm could be observed (Fig. 2c).

3.2 Tribological properties analysis

In order to evaluate the tribological properties of the MoS_2 nanospheres, experiments were conducted with varying loads and rotation speeds. In view of the previous work of our group [24], it has been found that when MoS_2 is with the mass ratio between 2% and 5%, there will be a better friction effect. Therefore, MoS_2 with the mass ratio of 3% has been chose in this research. Fig.3a represents the curve of friction of the HVI500 basic oil and the HVI500 oil containing 3 wt.% additives at the different loads (5N, 10N, 15N, 20N, 30N, 40N, 50N) under a speed of 300 rpm for 30 min. The friction coefficient of the HVI500 base oil without any additive increased with the load increasing. With the addition of 3.0 wt.% MoS_2 (Sample A) nanospheres in base oil, the friction coefficient was reduced remarkably when the load is less than 40 N. From these results, it can be concluded that the MoS_2 (Sample A) samples have better tribological capability. The spherical structure with nano-scale size will penetrate more easily into the interface with base oil and form thin oil film in the concave of rubbing face, which can decrease shearing stress, therefore resulted in a lower friction coefficient.

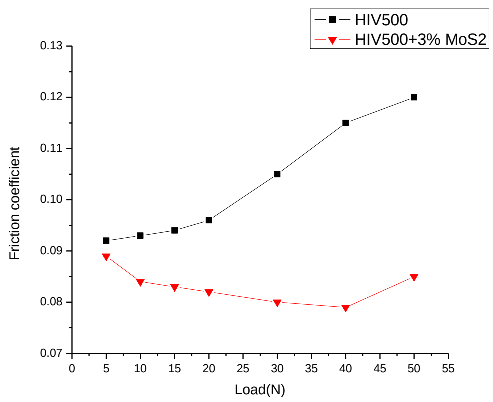

a

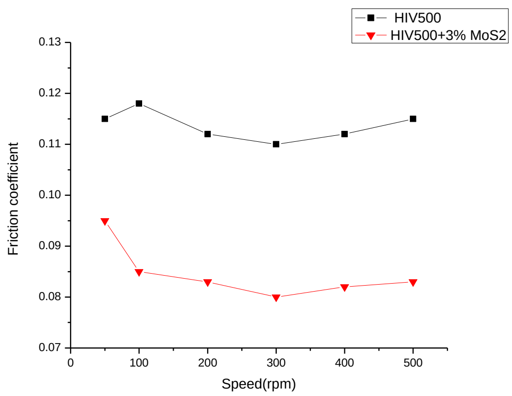

b

Fig. 3 a: Variations of friction coefficient of the HVI500 base oil and the base oil containing 3 wt.% MoS_2 nanospheres(Sample A) with increasing load at 300 rpm for 30 min. b:Curves of friction coefficient against rotational speed for the HVI500 base oil and the HVI500 base oil containing 3wt% MoS_2 nanospheres (Sample A) under 40 N load for 30 min

Fig.3b shows the comparisons of tribological properties among the HVI500 basic oil without additives and the base oil containing 3 wt.% MoS_2 (Sample A) nanospheres at the load of 40 N under diverse speeds. With the rotating speed of 50-500 rpm, the friction coefficient of the base oil containing prepared nanospheres is always lower than that of pure base oil, indication improved the friction reduction of the HVI500 base oil at different rotating speeds [25].

Fig.4 shows the comparisons of the tribological properties among the pure base oil and the base oil with different MoS_2 samples (sample A, B and C) at 40 N loads under a speed of 50 rpm. From the figure, it can be observed that the friction coefficient of the base oil containing three kinds of MoS_2 samples was lower than that of the HVI500 base oil. Furthermore, The base oil with MoS_2 (Sample A) nanospheres have lowest friction coefficient compared with others.

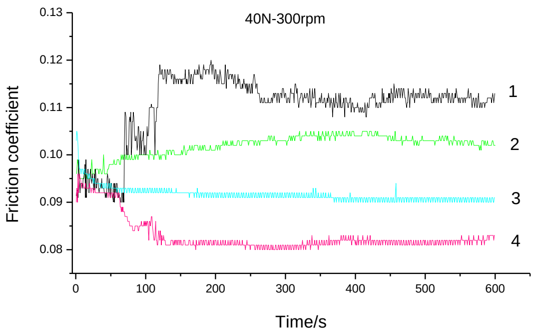

Fig. 4 Variation of friction coefficient for (a) the HVI500 base oil and the HVI500 base oil containing 3%$_{MoS2}$ at 40 N, 1: HVI500 2: 3%MoS_2 nanosheets (Sample B)+ HVI500 3: 3%MoS_2 microspheres (Sample C)+ HVI500 4:3%MoS_2 nanospheres (Sample A)+ HVI500

To further study the wear resistance tribological properties of the MoS_2 nanospheres, the topography of the worn scar was investigated using a SEM. The wear scar of the steel disc is shown in Fig. 5a (the HVI500 base oil) and Fig. 5b (the HVI500 base oil containing MoS_2 nanosphere) after rubbing with 40N load and 300 rpm rotating speed for 30min. It could easily be found from SEM image that the rubbed surface lubricated by the HVI500 base oil had lots of wide and deep furrows; Compared with the HVI500 base oil, the surface lubricated with MoS_2 nanospheres only presented slender furrows. Therefore, we believe MoS_2 nanospheres consist of many irregular nanosheets will penetrate more easily into the interface with the base oil, and these nanosheets could strongly adhere to substrates and form continuous film in concave of rubbing surface, enhancing the tribological properties [25].

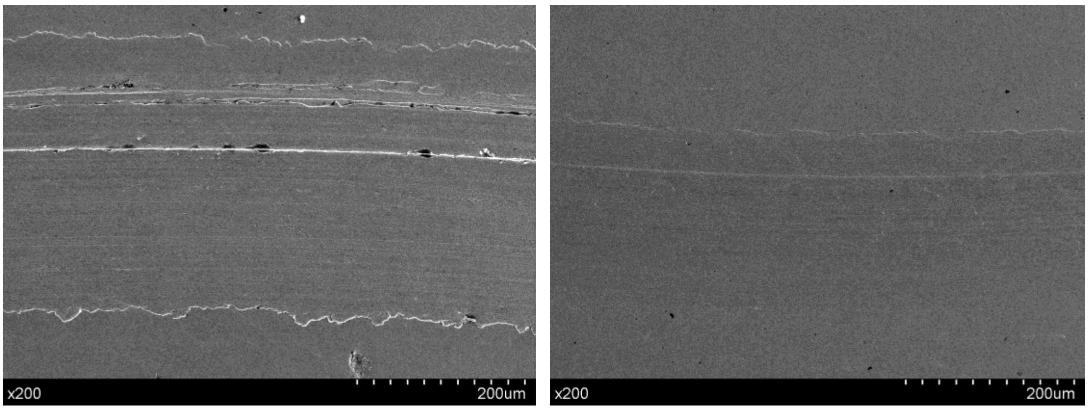

a b

Fig. 5 Wear scar of plate: (a)the HVI500 base oil, (b)the HVI500 base oil with 3.0 wt% MoS_2 nanospheres (Sample A)

5. Conclusions

In summary, We have successfully synthesized flower-like MoS_2 spheres with nanosheets by a facile solid-state reaction.Moreover, the MoS_2 nanospheres (sample A) showed better friction reduction performance than others did under the present experimental conditions. The differences of tribological properties are mainly ascribed to their morphology structures. The MoS_2 nanospheres could form a more stable tribofilm on the rubbing surface and improve the tribological properties of the base oil as a lubricant additive.

Acknowledgements

This work was financially supported by National Natural Science Foundation of China (51275213, 51302112), the Jiangsu National Nature Science Foundation (BK2011534, BK2011480), the Jiangsu Industry-University-Research Joint innovation Foundation (BY213065-05, BY213065-06) and Scientific and Technological Innovation Plan of Jiangsu Province in China (Grant Nos. CXLX12_0636).

References

[1] Tenne R. Adv. Mater. **7**, 965 (1995).
[2] Chianelli R.R, Prestridge E.B, Pecoraro T.A, ET AL. Science. **203**, 1105(1979).
[3] Tenne R., Nat, Nanotechnol. **1**,103 (2006).
[4] Tang G.G, Tang H, Li C.S., Li W.J, Ji X.R, Mater. Lett. **65**, 3457 (2011).
[5] Yu H.T, Liu Y, Brock S.L., Inorg. Chem. **47**, 1428 (2008).
[6] Chang.K, Chen W.X, J. Mater. Chem. **21**, 17175 (2011).
[7] Rapoport L, Bilik.Y, Feldman Y, Homyonfer M., ET AL. Nature. **38**, 7791(1997).
[8] Chhowalla M, Amaratunga G.A.J, Nature.**407**, 164 (2000).
[9] Uzcanga I, Bezverkhyy I., Afanasiev P, ET AL, Chem. Mater.**17**, 3575 (2005).
[10] Zelenski C.M, Dorhout P.K. J. Am. Chem. Soc.**120**, 734 (1998).
[11] Li X.L., Li Y.D, J. Phys. Chem. B.**108**, 1389 (2004).
[12] X.H. ZHANG, H. TANG, C.S. LI, Chalcogenide Letters. **10**, 403(2013).
[13] Y. Tian, Y. He, Y.F. Zhu, Mater. Chem. Phys. **87**, 87 (2004).
[14] F.L. Deepak, A. Mayoral, M.J. Yacaman, Mater. Chem. Phys. **118**, 392 (2009).
[15] F.L. Deepak, A. Mayoral, M.J. Yacaman, Appl. Phys. A Mater. Sci. Process. **96**, 861(2009).
[16] Y. Feldman, E. Wasserman, J. Srolovitz, R. Tenne, Science. **267**, 222 (1995).
[17] V.G. Pol, S.V. Pol, A. Gedanken, Cryst. Growth Des. **8**, 1126 (2008).
[18] Z.Z. Wu, D.Z. Wang, A.K. Sun, J. Cryst. Growth .**312**, 340 (2010).
[19] X. Zheng, L. Zhu, A. Yan, C. Bai, Y. Xie, Ultrason. Sonochem. **11**, 83 (2004).
[20] X.L. Li, J.P. Ge, Y.D. Li, Chem. Eur.J. **10**, 6163 (2004).
[21] R.H. Wei, H.B. Yang, K. Du, W.Y. Fu, Y.M. Tian, Q.J. Yu, S.K. Liu, M.H. Li, G.T. Zou, Mater. Chem.Phys. **108**, 188(2008).
[22] Yella A., Therese H.A., Zink N. Chem. Mater. **20**,587 (2008).

[23] G.G. Tang, J.R. Sun, W. Chen, H. Tang, Y. Wang, C.S. Li. Mater Lett. **100**,15 (2013).
[24] H.D. Huang, J.P. Tu, L.P. Gan, et al. Wear .**261**,140(2006).
[25] Zak A., Feldman Y., Alperovich V., AL.J. Am.Chem. Soc. **122**, 11108(2000).